ORIGINAL ARTICLE

GE ET AL.

NEED SHORT TITLE

**Discoidin Receptor 2 Controls Bone Formation and Marrow Adipogenesis***

Chunxi Ge,[1]* Zhengyan Wang,[2]* Guisheng Zhao,[1] Binbin Li,[4] Jinhui Liao,[2] Hanshi Sun,[1] and Renny T Franceschi[1,3]

[1]Departments of Periodontics and Oral Medicine and [2]Orthodontics and Pediatric Dentistry, University of Michigan School of Dentistry, Ann Arbor, MI, USA

[3]Department of Biological Chemistry, University of Michigan School of Medicine, Ann Arbor, MI, USA

[4]Department of Oral Pathology, Peking University School of Stomatology, Beijing, People's Republic of China

Author Manuscript

ABSTRACT

Cell–extracellular matrix (ECM) interactions play major roles in controlling progenitor cell fate and differentiation. The receptor tyrosine kinase, discoidin domain receptor 2 (DDR2), is an important mediator of interactions between cells and fibrillar collagens. DDR2 signals through both ERK1/2 and p38 MAP kinase, which stimulate osteoblast differentiation and bone formation. Here we show that DDR2 is critical for skeletal development and differentiation of marrow progenitor cells to osteoblasts while suppressing marrow adipogenesis. *Smallie* mice (*Ddr2*$^{slie/slie}$), which contain a nonfunctional *Ddr2* allele, have multiple skeletal defects. A progressive decrease in tibial trabecular bone volume/total volume (BV/TV) was observed when

wild-type (WT), *Ddr2*$^{wt/slie}$, and *Ddr2*$^{slie/slie}$ mice were compared. These changes were associated with reduced trabecular number (Tb.N) and trabecular thickness (Tb.Th) and increased trabecular spacing (Tb.Sp) in both males and females, but reduced cortical thickness only in *Ddr2*$^{slie/slie}$ females. Bone changes were attributed to decreased bone formation rather than increased osteoclast activity. Significantly, marrow fat and adipocyte-specific mRNA expression were significantly elevated in *Ddr2*$^{slie/slie}$ animals. Additional skeletal defects include widened calvarial sutures and reduced vertebral trabecular bone. To examine the role of DDR2 signaling in cell differentiation, bone marrow stromal cells (BMSCs) were grown under osteogenic and adipogenic conditions. *Ddr2*$^{slie/slie}$ cells exhibited defective osteoblast diversity and accelerated adipogenesis. Changes in differentiation were related to activity of runt-related transcription factor 2 (RUNX2) and PPARγ, transcription factors that are both controlled by MAPK-dependent phosphorylation. Specifically, the defective osteoblast disparity in calvarial cells from *Ddr2*$^{slie/slie}$ mice was associated with reduced ERK/MAP kinase and RUNX2-S319 phosphorylation and could be rescued with a constitutively active phosphomimetic RUNX2 mutant. Also, DDR2 was shown to increase RUNX2-S319 phosphorylation and transcriptional activity while also increasing PPARγ-S112 phosphorylation, but reducing its activity. DDR2 is, therefore, important for maintenance of osteoblast activity and suppression of marrow adipogenesis in vivo and these actions are related to changes in MAPK-dependent RUNX2 and PPARγ phosphorylation. © 2016 American Society for Bone and Mineral Research

Author Manuscript

**KEY WORDS:** GENETIC ANIMAL MODELS; TRANSCRIPTION FACTORS; OSTEOBLASTS; BONE–FAT INTERACTIONS

Received in original form December 30, 2015; revised form June 16, 2016; accepted June 22, 2016. Accepted manuscript online June 24, 2016.

Address correspondence to: Renny T. Franceschi, Department of Periodontics and Oral Medicine, University of Michigan School of Dentistry, 1011 N. University Ave., Ann Arbor, MI, USA. E-mail: rennyf@umich.edu

*CG and ZW contributed equally to this work.

Additional Supporting Information may be found in the online version of this article.

Journal of Bone and Mineral Research, Vol. XX, No. X, Month 2016, pp XXXX–XXXX

DOI: 10.1002/jbmr.2893

© 2016 American Society for Bone and Mineral Research

Author Manuscript

## Introduction

Extracellular matrix (ECM) signals have profound effects on the differentiation of many cell types. In bone, disparity of mesenchymal progenitor cells to osteoblasts requires interaction of progenitor cells with a type I collagen-containing ECM, a response that is in part mediated by $\alpha1\beta1$ and $\alpha2\beta1$ integrins.[1–4] However, the relatively mild bone phenotypes observed with knockout or inactivation of collagen-binding integrins in vivo suggest involvement of other collagen-binding molecules.[5,6]

Discoidin domain receptors (DDRs) are a second class of collagen receptors that differ from integrins in having intrinsic tyrosine kinase activity and selective affinity for triple-helical, native fibrillar and nonfibrillar collagens. DDR1 is of epithelial origin and has a broad ligand specificity, which includes all known collagens, whereas DDR2 is expressed by mesenchymal cells and principally binds collagens I, II, III, and X.[7,8] Both DDR1 and DDR2 participate in a broad

range of cell functions related to development, ECM turnover, growth regulation, and cancer (for reviews, see[7,9]). Two lines of genetic evidence suggest a role for DDR2 in bone. First, human *DDR2* mutations cause spondylo-meta-epiphyseal dysplasia (SMED), a skeletal disorder associated with dwarfism, short fingers, bowing of long bones, abnormal calcifications, and craniofacial abnormalities.[10,11] In addition, polymorphisms in *DDR2* are associated with low bone mineral density (BMD) and fracture risk in a Han Chinese population.[12] Mice harboring deletions in the *Ddr2* locus have a SMED-like phenotype characterized by dwarfism and reduction in total BMD.[13,14] However, the detailed bone phenotype of these animals has not been reported. Transgenic manipulation of *Ddr2* also affects body mass index (BMI) and adiposity,[14,15] suggesting possible additional effects of this receptor on energy metabolism.

Significantly, after collagen activation, DDR2 propagates downstream signals using the ERK1/2 and p38 MAP kinase pathways,[16,17] which are also required for normal skeletal development.[18–20] The ERK1/2 MAP kinase pathway affects osteoblast function by selectively phosphorylating runt-related transcription factor 2 (RUNX2), a key transcription factor controlling differentiation of osteoblast from mesenchymal progenitor cells. ERK1/2 binds and phosphorylates RUNX2 on several serine residues including S301 and S319, which are both required for RUNX2-dependent transcription.[21] These phosphorylation events are necessary for the response of bone to several important stimuli including ECM synthesis, mechanical loading, FGF2, and BMP treatment.[21–23] Similarly, PPARγ undergoes ERK-dependent phosphorylation at S112, resulting in decreased PPARγ transcriptional activity.[24] As we recently showed, activation of MAPK activity in mesenchymal cells both increases osteoblast distinction and suppresses adipogenesis, actions that require intact MAPK-dependent phosphorylation of RUNX2 and PPARγ.[25] These findings led us to hypothesize that DDR2 could also alter

Author Manuscript

osteoblast and adipocyte differentiation via MAPK-dependent phosphorylation. To test this hypothesis, we examined the bone and marrow fat phenotypes of *Ddr2*-deficient mice and showed that actions of DDR2 on osteoblast and adipocyte disparity can be explained by the selective regulation of RUNX2 and PPARγ.

**Materials and Methods**

Author Manuscript

## Animals

*Smallie* mice, which contain a spontaneous deletion in *Ddr2*, were initially obtained from the Jackson Laboratory on a C57BLS/J (BKS) background (*BKS(HRS-Ddr2$^{slie}$/JngJ*). Mice were bred with C57BL/J6 (B6) mice for at least 10 generations. Unlike mice on the BKS background that are sterile when homozygoic (*Ddr2$^{slie/slie}$*), homozygotes on the B6 background bred normally with normal litter sizes (results not shown). Nevertheless, mutant mice of both sexes retained the dwarf phenotype described on the BKS background (Supporting Fig. 1A–C). Female and male mice were genotyped using previously defined PCR primers and maintained on a normal chow diet until sacrifice at 3 or 5 months for analysis of skeletal and marrow fat phenotypes. Mice were used for skeletal analysis, RNA isolation and as a source of calvarial osteoblasts, marrow stromal cells (MSC), and marrow macrophage cultures. All animal studies were approved by the University of Michigan Committee on the Use and Care of Animals (UCUCA) and conformed to all guidelines and regulations for the protection of animal subjects. Mice were housed in specific pathogen-free Association for Assessment and Accreditation of Laboratory Animal Care ( AAALAC)-certified facilities. After genotyping, littermates were assigned to the experimental groups indicated.

## Micro–computed tomography analysis of bone

Trabecular and cortical bone parameters were measured by micro–computed tomography (μCT) using a Scanco Model 100 (Scanco Medical AG, Bassersdorf, Switzerland). Scan settings were: voxel size 12 μm, 70 kVp, 114 μA, 0.5 mm AL filter, and integration time 500 ms. All scans were analyzed using fixed thresholds (180 for trabecular bone and 280 for cortical bone). Trabecular parameters were collected from 50 sections (8 μm/section) under growth plates of

Author Manuscript

proximal tibia and the anterior end of L3 vertebrae. Cortical data were collected from 30 sections above trabecular bone of tibia and fibula junction.

Analysis of bone marrow fat accumulation

After μCT scanning and calculation of osseous parameters and an accurate marrow volume, samples were decalcified with 10% ethylenediaminetetraacetic acid. After fixation with 10% neutral buffered formalin for 24 hours, the samples were incubated with 1% osmium tetroxide at room temperature for 2 hours to stain marrow fat. Osmium staining was measured by μCT analysis.[26]

Dynamic histomorphometry and osteoclast analysis

For dynamic bone histomorphometry, 12-week-old mice were intraperitoneally injected with 30 mg/kg calcine 9 days before sacrifice and then with 10 mg/kg Alizarin Red 2 days before sacrifice. Tibias were harvested and embedded with methyl methacrylate. Six micron sections were cut using a Leica SM2500 metallurgical cutting system. For the measurement of in vivo osteoclast activity, tibias were harvested from 12-week-old mice. Tartrate-resistant acid phosphatase (TRAP) staining was performed on histological sections using the Sigma Trap staining kit (387-A). The fluorescence and TRAP stained images were photographed using a Nikon 50i microscope. Histomorphometric parameters for double labels and osteoclast activity were assessed using an OsteoMeasureXP system (OsteoMetrics, Decatur, GA, USA).

Cell cultures and in vitro differentiation

Primary calvaria osteoblasts and bone marrow stromal cells (BMSCs) were isolated from 12-week-old mice as previously described.[27–29] Osteoblast differentiation was induced by growth in

Author Manuscript

α modified essential medium/10% fetal bovine serum (α-MEM/10% FBS) containing 50 μg/mL ascorbic acid and 10 mM β-glycerophosphate. For adipogenesis, cells were grown for 2 days in α-MEM containing 10% FBS, insulin (5 μg/mL), dexamethasone (1 μM), IBMX (500 μM), and troglitazone (5 μM), followed by growth in a medium containing troglitazone (5 μM) for 9 days. To stain mineral, cells were incubated at room temperature in 2% Alizarin Red S (pH 4.2 with 10% ammonium hydroxide) for 0.5 hours. For measurement of fat-droplet accumulation, fixed cells were incubated with 60% isopropyl alcohol for 10 min, then stained with 2 mg/mL Oil Red O for 1 hour. For in vitro osteoclast differentiation, bone marrow macrophages (BMM) were isolated from tibias and femurs of 12-week-old mice using the method of Mizoguchi and coworkers[30] and treated with 10 ηg/mL M-CSF and 50 ηg/mL RANKL for 3 days.[31] For measurement of osteoclast induction, cells were stained for TRAP (Sigma staining kit; Sigma-Aldrich, St. Louis, MO, USA) or grown on BioCoat Osteologic dishes (BD Biosciences, San Jose, CA, USA) for 3 days before measurement of pit formation. Cell images were taken using an inverted phase contrast microscope (Nikon D300). Osteoblasts and adipocyte-specific mRNA expression were assessed by real-time RT-PCR and normalized to GAPDH as previously described.[25] The following mRNAs were measured: *Bglap2*, *Ibsp*, and *Runx2* mRNAs for osteoblasts and *Pparg*, *Cebpa*, *Adipoq*, and *Fabp4* for adipocytes. Western blot analysis was performed using standard procedures. Sources for antibodies were as follows: total RUNX2 antibody, MBL; PPARγ phospho-S112-specific antibody and total PPARγ antibody, Millipore; phospho-ERK1/2 and total ERK1/2 antibody, Cell Signaling. RUNX2 phospho-S319-specific antibody was previously described.[22] Phosphorylation at this site is closely correlated with overall levels of RUNX2 transcriptional activity.[21,22]

Author Manuscript

Transfections

The 6OSE2-Luc reporter, pCMV wild-type (WT) RUNX2 (RUNX2-WT), S301,319A RUNX2 (RUNX2-SA), and S301,319E RUNX2 (RUNX2-SE) expression vectors were previously described,[21] as were ARE-Luc, RXR, wild-type PPARγ (PPARγ-WT) and S112A PPAR $\gamma$ vectors (PPARγ-SA).[32,33] WT, dominant-negative, and constitutively active DDR2 expression vectors were a generous gift from Dr. Scott Friedman, Mt. Sinai School of Medicine, New York, NY, USA.[34] For lentivirus production, cDNAs encoding WT RUNX2, RUNX2-SA, or RUNX2-SE were subcloned into pLenti-GFP-puro (Addgene #17448) and packaged by the University of Michigan Vector Core, Ann Arbor, MI, USA. Calvarial cells were isolated from 12-week-old WT and *Ddr2*$^{slie/slie}$ mice, transduced with lentivirus vectors, and stable cell lines were developed by selection in 100 μg/mL puromycin for 4 weeks. To measure effects of DDR2 on RUNX2 and PPARγ transcriptional activity, COS7 cells were transfected with the indicated expression plasmids and either 6OSE2-Luc (RUNX2 reporter) or PPRE-Luc (PPARγ reporter), and pRL-SV40 (encodes Renilla reniformis luciferase to control for transfection efficiency), as previously described.[25]

Statistical analysis

All statistical analyses were performed using SPSS version 16.0 Software (SPSS, Inc., Chicago, IL, USA). Unless indicated otherwise, each reported value is the mean ± SD of triplicate independent samples for in vitro cultures or at least six animals per group for in vivo studies. Statistical significance was assessed using a one-way analysis of variance.

**Results**

Author Manuscript

Reduced trabecular bone in the appendicular and axial skeletons of *Ddr2*$^{slie/slie}$ mice is explained by a selective defect in bone formation

*Smallie* mice contain a 150-kilobase (kb) deletion in the *Ddr2* locus that includes most of the coding sequence (17 out of 18 exons deleted), resulting in a loss of function allele.[14] Like SMED patients, these animals are dwarfed and have reduced total bone mass but, otherwise, their bone phenotype has not been characterized. To further define the skeletal phenotype of *Smallie* mice, µCT was used to examine tibias from WT, *Ddr2*$^{wt/slie}$, and *Ddr2*$^{slie/slie}$ animals. Tibias of 3- and 5-month-old mice showed major decreases in trabecular bone that were proportional to gene dose in both genders (females in Supporting Fig. 2 and Fig. 1, and males in Supporting Fig. 3). For example, in 5-month-old females *Ddr2*$^{wt/slie}$ mice exhibited a 35% decrease in bone volume/total volume (BV/TV) relative to WT controls, whereas this parameter was decreased nearly 70% in *Ddr2*$^{slie/slie}$ animals (Fig. 1*B*). These changes were accompanied by expected reductions in trabecular number (Tb.N) and thickness (Tb.Th), and increased trabecular spacing (Tb.Sp) (Fig. 1*C–E*). In addition, a 7% decrease in cortical bone was observed in females, but not in males (compare Fig. 1*F* with Supporting Fig. 3F). Changes in bone mass were accompanied by a gene dosage-related decline in mineral apposition rate (MAR) and bone formation rate (BFR) (Fig. 1*G–I*), osteoblast marker (*Runx2, Bglap2,* and *Ibsp*) mRNA levels (Fig. 1*J–L*), and serum osteocalcin when *Ddr2*$^{wt/slie}$ and *Ddr2*$^{slie/slie}$ mice were compared with WT (Fig. 1*M*). *Ddr2*$^{slie/slie}$ mice also had large reductions in vertebral trabecular bone. Micro–computed tomography analysis of the third lumbar vertebrae revealed 20% and 60% declines in BV/TV in *Ddr2*$^{wt/slie}$ and *Ddr2*$^{slie/slie}$ mice, respectively (Supporting Fig. 4).

<Insert Figure 1>

Author Manuscript

Two approaches were used to determine if the decreased bone in *Ddr2*$^{slie/slie}$ mice was in part explained by changes in bone resorption: (1) TRAP staining was used to measure osteoclast surface and numbers in tibia; and (2) the ability of bone marrow macrophage cultures to undergo osteoclast differentiation was measured. No differences were seen in osteoclast surface, osteoclast number, or osteoclast number/osteoclast surface. In addition, the serum bone resorption markers CTx-1 and TRAP were not affected by *Ddr2* status (Supporting Fig. 5A–F). Furthermore, after growth of BMM in medium containing M-CSF and RANKL to induce osteoclast formation, no differences were observed between groups in terms of TRAP-positive cells/dish or mineral resorption measured using BioCoat dishes (Supporting Fig. 6A–D). Finally, equivalent levels of two osteoclast marker mRNAs, *Ctsk* and *Nfatc1*, and culture medium levels of CTx-1 and TRAP were detected in all groups (Supporting Fig. 6E–H). Thus *Ddr2* deletion in vivo preferentially affects bone formation without noticeably altering osteoclast activity.

The reduced bone in *Ddr2*$^{slie/slie}$ mice is associated with increased marrow fat

Histological examination of bones from *Ddr2*$^{wt/slie}$ and *Ddr2*$^{slie/slie}$ mice often showed regions containing apparent adipocytes (Supporting Fig. 5A). To quantify this marrow fat, tibia from 5-month-old female mice were stained with the lipophilic compound osmium tetroxide, and tibial marrow fat was visualized by μCT.[26] As shown in Fig. 2, marrow fat increased in proximal and distal regions. Specific quantitation of osmium density in the proximal tibia revealed a more than fivefold increase in marrow adipose tissue when WT, *Ddr2*$^{wt/slie}$ and *Ddr2*$^{slie/slie}$ mice were compared (Fig. 2*B–D*). Gene expression profiles of whole bone also confirmed a shift from osteoblast (*Runx2*, *Bglap2*, *Ibsp*) to adipocyte (*Pparg*, *Cebpa*, *Fabp4*, and *Adipoq*) marker

Author Manuscript

mRNAs (compare Fig. 1*J–L* with Fig. 2*E–H*). In addition, serum adiponectin levels increased in parallel with *Adipoq* mRNA, whereas serum leptin decreased (Fig. 2*I*, *J*).

<Insert Figure 2>

Impaired osteoblast differentiation and increased adipogenesis in BMSCs from *Ddr2*$^{slie/slie}$ mice

To determine the requirement for DDR2 in the distinction of marrow progenitors to osteoblasts or adipocytes, BMSCs from WT and *Ddr2*$^{slie/slie}$ mice were grown in osteoblast or adipocyte induction conditions (Fig. 3). Cells from *Ddr2*$^{slie/slie}$ mice formed fewer mineralized nodules and expressed lower levels of osteoblast marker mRNAs (Fig. 3*A–D*). In contrast, they formed increased numbers of lipid droplet-containing cells and expressed higher levels of adipocyte markers (Fig. 3*E–I*). Although DDR2 has been reported to affect cell proliferation in other cell types such as fibroblasts, no major differences in proliferation rates were observed when BMSCs from wild-type and *Ddr2*$^{slie/slie}$ mice were compared (Supporting Fig. 1D).

<Insert Figure 3>

Defective calvarial mineralization and osteoblasts contrast in *Ddr2*$^{slie/slie}$ mice

In addition to the defects in the appendicular and axial skeleton noted above, skulls from newborn *Ddr2*$^{slie/slie}$ mice had widened sutures and were poorly mineralized, such that total cranial bone volume was reduced by approximately 40% (Fig. 4*A*, *B*). In addition, calvarial osteoblasts from these mice, like BMSCs, formed few mineralized nodules and expressed lower levels of osteoblast marker mRNAs than cells from WT littermates (Fig. 4*C–F*).

Basis for DDR2 effects on osteoblast and adipocyte differences

Author Manuscript

MAPK activation in mesenchymal cells both increases osteoblast differences and inhibits adipogenesis via phosphorylation of RUNX2 and PPARγ.[22] Because MAPK is a major DDR2-activated downstream signal,[16,17] we hypothesized that reduced MAPK signaling in DDR2-deficient cells could explain the observed decrease in osteoblast differentiation and increase in adipogenesis. This hypothesis was evaluated in two ways. We: (1) examined the role of RUNX2 phosphorylation in the differentiation of calvarial cells from WT and DDR2-deficient mice; and (2) directly measured the ability of DDR2 to regulate RUNX2 and PPARγ phosphorylation and transcriptional activity.

In agreement with our previous report,[22] MAP kinase activity (P-ERK/total ERK) and RUNX2 phosphorylation (P-RUNX2/total RUNX2) gradually increased during calvarial osteoblast differentiation. This increase was accompanied by a parallel increase in DDR2 protein (Fig. 4*G–I*). Consistent with their reduced differentiation potential, DDR2-deficient cells had much lower levels of MAP kinase activity and RUNX2 phosphorylation. To determine if this could explain the observed suppression of osteoblast diversity in cells from *Ddr2*$^{slie/slie}$ mice, we compared the activity of WT (RUNX2-WT), phosphorylation site mutant (RUNX2 S301,S319A; RUNX2-SA), and phosphorylation site mimetic (RUNX2 S301,S319E; RUNX2-SE) forms of RUNX2 in WT or DDR2-deficient cells (Fig. 4*J–L*). Lentiviral transduction was used to generate stable cell lines that were then grown in osteoblast disparate conditions for 2 weeks before measurement of osteoblast mRNAs. Consistent with previous findings,[21] overexpression of WT RUNX2 in DDR2-sufficient (WT) cells strongly induced *Ibsp* and *Bglap*2 mRNAs, whereas levels were reduced by approximately 50% in cells expressing the phosphorylation-deficient mutant (RUNX2-SA). As would be expected if RUNX2 phosphorylation was necessary for DDR2 effects on differentiation, mRNA levels were reduced to similar levels in DDR2-deficient

Author Manuscript

(DDR2) cells regardless of whether they were expressing WT or phosphorylation-deficient RUNX2. Similarly, in cells expressing the phosphorylation mimetic RUNX2 (RUNX2-SE), which does not require phosphorylation for full activity, both *Bgalp2* and *Ibsp* mRNAs were expressed at high levels regardless of DDR2 status.

<Insert Figure 4>

Effects of DDR2 on RUNX2 and PPARγ transcriptional activity measured using luciferase reporters are shown in Fig. 5. In cells transfected with WT RUNX2, WT DDR2 and, to a greater extent, a constitutively active DDR2 mutant increased RUNX2 phosphorylation (P-RUNX2/total RUNX2) and transcriptional activity whereas a dominant-negative DDR2 mutant had no effect (Fig. 5*A*, *B*). As expected, DDR2 also increased MAPK activity (P-ERK) without affecting either total RUNX2 or ERK levels. The RUNX2 response required MAPK-dependent phosphorylation because the RUNX2-SA mutant was resistant to DDR2 regulation. Similarly, DDR2 actions on PPARγ transcriptional activity are explained by a mechanism involving MAPK-dependent phosphorylation (Fig. 5*C*, *D*). In this case, a WT or constitutively active DDR2 increased PPARγ S112 phosphorylation with concomitant inhibition of reporter activity whereas a dominant-negative mutant was inactive. In contrast PPARγ, containing an S112A mutation rendering it resistant to MAPK-dependent inhibition, had higher basal activity and was not inhibited by DDR2 overexpression.

<Insert Figure 5>

Author Manuscript

**Discussion**

Here we describe the skeletal and marrow fat phenotypes of *Ddr2*-deficient mice and relate these changes to defects in MAP kinase signaling and phosphorylation of RUNX2 and PPARγ.

Although absence of DDR2 inhibits growth and body size, effects previously attributed to reduced proliferation of growth plate chondrocytes,[13] our studies clearly show that DDR2 is also required for normal trabecular bone formation in the absence of changes in resorption. Furthermore, loss of DDR2 increases marrow adipogenesis and alters serum levels of the adipocyte-related hormones adiponectin and leptin.

This study provides the first in vivo evidence that DDR2 increases bone mass largely by increasing osteoblast differentiation and bone formation. Specifically, bone formation in *Ddr2*$^{slie/slie}$ mice was shown to be dramatically reduced, leading to decreased trabeculae in long bones and vertebrae. Consequently, osteoblast differentiation was reduced in BMSCs and calvarial cells from *Ddr2*-deficient mice due to a reduction in ERK/MAP kinase signaling and RUNX2 phosphorylation. The concept that DDR2 stimulates bone formation through MAP kinase and RUNX2 was originally proposed by Zhang and coworkers on the basis of studies with osteoblast and chondrocyte cell lines.[35] In their study, DDR2 was shown to increase MAP kinase activity and phosphorylation of RUNX2 at Ser 301 and Ser 319,[35] sites previously identified by us as being essential for MAPK-dependent RUNX2 transcriptional activity.[21] More recently, the same group proposed, largely on the basis of cell culture studies, that DDR2 can also suppress osteoclastogenesis and showed that overexpression of DDR2 in bone marrow could reverse ovariectomy-induced bone loss.[36] Whereas our studies provide in vivo validation of the former concept, we failed to obtain evidence for defective osteoclast formation in *Ddr2*$^{slie/slie}$ mice. These animals had normal levels of bone-associated osteoclasts and serum resorption markers. Furthermore, osteoclast differentiation from bone marrow macrophages as measured by induction of osteoclast markers or bone resorbing activity (resorptive pit formation) was normal, indicating that the principal in vivo effects of DDR2 on bone are at the level of

osteoblast differentiation and bone formation. Although it is difficult to directly compare our in vivo results with this previous work, a possible reason for this apparent discrepancy might be compensation for loss of DDR2 when it is absent during all stages of osteoclast development in vivo that does not occur when DDR2 is knocked down with shRNA during differentiation of osteoclasts in vitro.

In the initial report describing *Ddr2*$^{slie/slie}$ mice, homozygous animals were found to be sterile due to gonadal insufficiency in both males and females.[14] Although all pituitary and hypothalamic hormones and releasing factors were normal as was circulating IGF-1, secreted steroid hormones were reduced in both genders. Clearly, reduced steroid hormone levels would be expected to affect bone metabolism as well as reproduction. Nevertheless, we do not think this explains our results. As noted in Materials and Methods, when originally characterized, *smallie* mice were on a BKS background; all our studies used B6 mice, which bred normally even as *Ddr2*$^{slie/slie}$ homozygotes (see Materials and Methods). Although we have not measured circulating steroid hormone levels, they are indeed sufficient for gender maturation and function. Moreover, our failure to observe defects in osteoclastogenesis in females is certainly incompatible with a major reduction in gender steroids. Thus the reproductive defects associated with the absence of DDR2 are likely mouse line-specific. Nonetheless, a more detailed understanding of the functions of DDR2 in bone will require the development of a tissue-specific knockout model that is currently under development in our laboratory.

Our observation that marrow adipose tissue is dramatically increased in *Ddr2*$^{slie/slie}$ mice is of particular interest, in that marrow adiposity is associated with many skeletal diseases including osteoporosis and disuse osteopenia.[37–39] Previous analysis of *Ddr2*$^{slie/slie}$ mice detected a modest decrease in total body fat in males and females and significantly elevated blood glucose

Author Manuscript

levels. However, marrow fat was not examined.[14] Paradoxically, transgenic overexpression of *Ddr2* in all tissues also decreased BMI and epididymal fat pad weight while decreasing serum LDL-cholesterol, albumin, and uric acid but, again, marrow fat was not analyzed.[15]

As we recently showed, differentiation of mesenchymal cells into osteoblasts or adipocytes is reciprocally controlled by the relative activity of RUNX2 and PPARγ, transcription factors that are both regulated by MAP kinase-dependent phosphorylation.[25] Specifically, phosphorylation of RUNX2 at Ser 301 and Ser 319 increases transcriptional activity and osteoblast differentiation, whereas phosphorylation of PPARγ at Ser 112 inhibits its activity and blocks adipogenesis. This pathway provides a plausible mechanism to explain how DDR2, acting through MAP kinase, increases bone formation and suppresses marrow adipogenesis. As shown in Fig. 5, DDR2 stimulates phosphorylation of both RUNX2 and PPARγ leading to increased RUNX2-dependent transcriptional activity and decreased PPARγ-dependent transcription. Also, as would be predicted, MAP kinase activity, RUNX2 phosphorylation, and osteoblast differentiation are reduced in calvarial cultures from *Ddr2*$^{slie/slie}$ mice. The decreased osteoblast differentiation in DDR2-deficient cells was explained by a defect in RUNX2 phosphorylation that was likely a consequence of the reduced MAPK activity in these cells; differences in RUNX2-dependent gene expression in wild-type versus DDR2-deficient cells were not seen in cells containing a phosphorylation-deficient RUNX2 mutant (RUNX2 S301,319A), whereas a phosphomimetic mutant (RUNX2 S301,319E) restored transcriptional activity to the same levels in wild-type or DDR2-deficient cells (Fig. 4*J–L*).

Notably, MAPK activity, RUNX2 phosphorylation, and osteoblast differentiation are only partially inhibited in cells from *Ddr2*$^{slie/slie}$ mice (Fig. 4*G–I*). This indicates that DDR2 is not the only mediator of the collagen/MAPK/RUNX2 pathway in bone cells. As mentioned in the

Author Manuscript

Introduction, collagen-binding integrins can also stimulate osteoblast disparity and they likely account for the residual osteoblast distinction and bone formation in the absence of DDR2.

The observation that DDR2 can affect peripheral and marrow fat, as well as the adipokines adiponectin and leptin, proposes that DDR2 may also participate in the regulation of energy metabolism, possibly through its action on marrow adipose tissue. Recent studies showed that marrow fat is a major source of circulating adiponectin and manipulations that alter marrow adiposity can also affect adiponectin levels.[40] Accordingly, it is possible that the increased serum adiponectin we observed in *Ddr2*$^{slie/slie}$ mice may be related to the increased marrow adipose tissue in these animals and that changes in adiponectin may explain the reported decrease in BMI in the absence of DDR2.[14] Nevertheless, further studies will be required to establish a direct role for DDR2 in energy metabolism.

Author Manuscript

**Disclosures**

All authors state that they have no conflicts of interest.

**Acknowledgments**

This work was supported by NIDCR Grants DE11723 (RTF), K12 DE023574 (Junior Faculty Training Award, CG), and NIDDK Grant P30 DK092926 (Michigan Center for Diabetes Translational Research).

Authors' roles: Study design: CG and RTF. Conducting of experiments: CG, ZW, GZ, BL, JL, and HS. Writing of manuscript: RTF and CG. Proofreading and approving final version of manuscript: All authors.

**References**

1. Xiao G, Wang D, Benson MD, Karsenty G, Franceschi RT. Role of the alpha2-integrin in osteoblast-specific gene expression and activation of the Osf2 transcription factor. J Biol Chem. 1998;273(49):32988–94.

2. Xiao G, Gopalakrishnan R, Jiang D, Reith E, Benson MD, Franceschi RT. Bone morphogenetic proteins, extracellular matrix, and mitogen-activated protein kinase signaling pathways are required for osteoblast-specific gene expression and differentiation in MC3T3-E1 cells. J Bone Miner Res. 2002;17(1):101–10.

3. Takeuchi Y, Suzawa M, Kikuchi T, Nishida E, Fujita T, Matsumoto T. Differentiation and transforming growth factor-beta receptor down-regulation by collagen-alpha2beta1 integrin interaction is mediated by focal adhesion kinase and its downstream signals in murine osteoblastic cells. J Biol Chem. 1997;272(46):29309–16.

4. Reyes CD, Garcia AJ. Alpha2beta1 integrin-specific collagen-mimetic surfaces supporting osteoblastic differentiation. J Biomed Mater Res A. 2004;69(4):591–600.

5. Zimmerman D, Jin F, Leboy P, Hardy S, Damsky C. Impaired bone formation in transgenic mice resulting from altered integrin function in osteoblasts. Dev Biol. 2000;220(1):2–15.

6. Gardner H, Broberg A, Pozzi A, Laato M, Heino J. Absence of integrin alpha1beta1 in the mouse causes loss of feedback regulation of collagen synthesis in normal and wounded dermis. J Cell Sci. 1999;112(Pt 3):263–72.

Author Manuscript

7. Fu HL, Valiathan RR, Arkwright R, et al. Discoidin domain receptors: unique receptor tyrosine kinases in collagen-mediated signaling. J Biol Chem. 2013;288(11):7430–7.

8. Leitinger B, Kwan AP. The discoidin domain receptor DDR2 is a receptor for type X collagen. Matrix Biol. 2006;25(6):355–64.

9. Valiathan RR, Marco M, Leitinger B, Kleer CG, Fridman R. Discoidin domain receptor tyrosine kinases: new players in cancer progression. Cancer Metastasis Rev. 2012;31(1-2):295–321.

10. Bargal R, Cormier-Daire V, Ben-Neriah Z, et al. Mutations in DDR2 gene cause SMED with short limbs and abnormal calcifications. Am J Hum Genet. 2009;84(1):80–4.

11. Al-Kindi A, Kizhakkedath P, Xu H, et al. A novel mutation in DDR2 causing spondylo-meta-epiphyseal dysplasia with short limbs and abnormal calcifications (SMED-SL) results in defective intra-cellular trafficking. BMC Med Genet. 2014;15:42.

12. Guo Y, Yang TL, Dong SS, et al. Genetic analysis identifies DDR2 as a novel gene affecting bone mineral density and osteoporotic fractures in Chinese population. PLoS One. 2015;10(2):e0117102.

13. Labrador JP, Azcoitia V, Tuckermann J, et al. The collagen receptor DDR2 regulates proliferation and its elimination leads to dwarfism. EMBO Rep. 2001;2(5):446–52.

Author Manuscript

14. Kano K, Marin de Evsikova C, Young J, et al. A novel dwarfism with gonadal dysfunction due to loss-of-function allele of the collagen receptor gene, Ddr2, in the mouse. Mol Endocrinol. 2008;22(8):1866–80.

15. Kawai I, Matsumura H, Fujii W, et al. Discoidin domain receptor 2 (DDR2) regulates body size and fat metabolism in mice. Transgenic Res. 2014;23(1):165–75.

16. Ruiz PA, Jarai G. Collagen I induces discoidin domain receptor (DDR) 1 expression through DDR2 and a JAK2-ERK1/2-mediated mechanism in primary human lung fibroblasts. J Biol Chem. 2011;286(15):12912–23.

17. Zhang K, Corsa CA, Ponik SM, et al. The collagen receptor discoidin domain receptor 2 stabilizes SNAIL1 to facilitate breast cancer metastasis. Nat Cell Biol. 2013;15(6):677–87.

18. Ge C, Xiao G, Jiang D, Franceschi RT. Critical role of the extracellular signal-regulated kinase-MAPK pathway in osteoblast differentiation and skeletal development. J Cell Biol. 2007;176(5):709–18.

19. Matsushita T, Chan YY, Kawanami A, Balmes G, Landreth GE, Murakami S. Extracellular signal-regulated kinase 1 (ERK1) and ERK2 play essential roles in osteoblast differentiation and in supporting osteoclastogenesis. Mol Cell Biol. 2009;29(21):5843–57.

Author Manuscript

20. Greenblatt MB, Shim JH, Zou W, et al. The p38 MAPK pathway is essential for skeletogenesis and bone homeostasis in mice. J Clin Invest. 2010;120(7):2457–73.

21. Ge C, Xiao G, Jiang D, et al. Identification and functional characterization of ERK/MAPK phosphorylation sites in the Runx2 transcription factor. J Biol Chem. 2009;284(47):32533–43.

22. Ge C, Yang Q, Zhao G, Yu H, Kirkwood KL, Franceschi RT. Interactions between extracellular signal-regulated kinase 1/2 and p38 MAP kinase pathways in the control of RUNX2 phosphorylation and transcriptional activity. J Bone Miner Res. 2012;27(3):538–51.

23. Li Y, Ge C, Long JP, et al. Biomechanical stimulation of osteoblast gene expression requires phosphorylation of the RUNX2 transcription factor. J Bone Miner Res. 2012;27:1263–74.

24. Hu E, Kim JB, Sarraf P, Spiegelman BM. Inhibition of adipogenesis through MAP kinase-mediated phosphorylation of PPARgamma. Science. 1996;274(5295):2100–3.

25. Ge C, Cawthorn WP, Li Y, Zhao G, MacDougald OA, Franceschi RT. Reciprocal control of osteogenic and adipogenic differentiation by ERK/MAP kinase phosphorylation of Runx2 and PPARgamma transcription factors. J Cell Physiol. 2016;231(3):587–96.

26. Fretz JA, Nelson T, Xi Y, Adams DJ, Rosen CJ, Horowitz MC. Altered metabolism and lipodystrophy in the early B-cell factor 1-deficient mouse. Endocrinology. 2010;151(4):1611–21.

Author Manuscript

27. Ducy P, Karsenty G. Two distinct osteoblast-specific cis-acting elements control expression of a mouse osteocalcin gene. Mol Cell Biol. 1995;15(4):1858–9.

28. Krebsbach PH, Mankani MH, Satomura K, Kuznetsov SA, Robey PG. Repair of craniotomy defects using bone marrow stromal cells. Transplantation. 1998;66(10):1272–8.

29. Rim JS, Mynatt RL, Gawronska-Kozak B. Mesenchymal stem cells from the outer ear: a novel adult stem cell model system for the study of adipogenesis. FASEB J. 2005;19(9):1205–7.

30. Mizoguchi T, Muto A, Udagawa N, et al. Identification of cell cycle-arrested quiescent osteoclast precursors in vivo. J Cell Biol. 2009;184(4):541–54.

31. Yamashita J, Datta NS, Chun YH, et al. Role of Bcl2 in osteoclastogenesis and PTH anabolic actions in bone. J Bone Miner Res. 2008;23(5):621–32.

32. Camp HS, Tafuri SR. Regulation of peroxisome proliferator-activated receptor gamma activity by mitogen-activated protein kinase. J Biol Chem. 1997;272(16):10811–6.

33. Perez A, Kastner P, Sethi S, Lutz Y, Reibel C, Chambon P. PMLRAR homodimers: distinct DNA binding properties and heteromeric interactions with RXR. EMBO J. 1993;12(8):3171–82.

Author Manuscript

34. Olaso E, Labrador JP, Wang L, et al. Discoidin domain receptor 2 regulates fibroblast proliferation and migration through the extracellular matrix in association with transcriptional activation of matrix metalloproteinase-2. J Biol Chem. 2002;277(5):3606–13.

35. Zhang Y, Su J, Yu J, et al. An essential role of discoidin domain receptor 2 (DDR2) in osteoblast differentiation and chondrocyte maturation via modulation of Runx2 activation. J Bone Miner Res. 2011;26(3):604–17.

36. Zhang Y, Su J, Wu S, et al. DDR2 (discoidin domain receptor 2) suppresses osteoclastogenesis and is a potential therapeutic target in osteoporosis. Sci Signal. 2015;8(369):ra31.

37. Justesen J, Stenderup K, Ebbesen EN, Mosekilde L, Steiniche T, Kassem M. Adipocyte tissue volume in bone marrow is increased with aging and in patients with osteoporosis. Biogerontology. 2001;2(3):165–71.

38. Meunier P, Aaron J, Edouard C, Vignon G. Osteoporosis and the replacement of cell populations of the marrow by adipose tissue. A quantitative study of 84 iliac bone biopsies. Clin Orthop Relat Res. 1971;80:147–54.

39. Minaire P, Edouard C, Arlot M, Meunier PJ. Marrow changes in paraplegic patients. Calcif Tissue Int. 1984;36(3):338–40.

Author Manuscript

40. Cawthorn WP, Scheller EL, Learman BS, et al. Bone marrow adipose tissue is an endocrine organ that contributes to increased circulating adiponectin during caloric restriction. Cell Metab. 2014;20(2):368–75.

**Fig. 1.** Decreased trabecular and cortical bone, bone formation, and osteoblast gene expression in *Ddr2*$^{slie/slie}$ mice. Trabecular and cortical bone parameters were measured by μCT in 5-month-old *Ddr2*$^{wt/wt}$ (wild-type [WT]), *Ddr2*$^{slie/wt}$ (hetero), or *Ddr2*$^{slie/slie}$ (homo) female mice. (*A*) Representative μCT images of tibia showing trabecular and cortical bone. (*B–E*) Measurements are shown for trabecular bone volume over total volume (BV/TV), trabecular number (Tb.N), trabecular thickness (Tb.Th, mm) and trabecular spacing (Tb.Sp, mm). (*F*) Cortical BV/TV. (*G–I*) Dynamic bone histomorphometry. For measurement of bone formation parameters, 12-week-old female mice were injected with calcine and Alizarin Red followed by measurement of mineral apposition rate (MAR) and bone formation rate (BFR). Representative fluorescent images are shown in (*G*). (*J–L*) Osteoblast marker mRNAs. RNA was extracted from whole bones of 5-month-old females and the following mRNAs were measured: *Runx2, Bglap2,* and *Ibsp*. (*M*) Serum levels of total osteocalcin (Bglap2). $n = 8$/group; statistically significant at $^*p < 0.01$.

**Fig. 2.** Increased marrow adipose tissue in tibias from 5-month-old female *Ddr2*$^{slie/slie}$ mice. Analysis used the same samples as Fig. 1*A–F*. (*A*) Micro–CT images of osmium-stained demineralized tibias from wild-type (WT), heterozygous, and homozygous *Ddr2*$^{slie/slie}$ mice showing landmarks used to calculate multifocal atrial tachycardia (MAT) in the proximal tibias (dashed lines). (*B–D*) Measurement of total osmium-positive volume (OSM, $mm^3$), total bone volume (TV, $mm^3$), and osmium-positive volume/total bone volume (OSM/TV). (*E–H*) Adipocyte marker mRNA levels from whole bone: *Pparg* mRNA (*E*), *Cebpa* mRNA (*F*), *Fabp4* mRNA (*G*), and *Adipoq* mRNA (*H*). (*I, J*) Measurement of serum adipocyte marker proteins by ELISA: adiponectin (*I*) and leptin (*J*). $n = 8$/group; statistically significant at $^*p < 0.01$.

Fig. **3.** Decreased osteoblast and increased adipocyte differentiation in BMSCs from *Ddr2*$^{slie/slie}$ mice. BMSCs were isolated from 12-week-old wild-type (WT) and homozygous *Ddr2*$^{slie/slie}$ female mice (DDR2) and grown in osteogenic (*A–D*), or adipogenic conditions (*E–I*). (*A*) Mineralization. Cells were stained with Alizarin Red after 3 weeks in culture. (*B–D*) Osteoblast differentiation marker mRNAs: (*B*) *Runx2* mRNA, (*C*) *Bglap2* mRNA, and (*D*) *Ibsp* mRNA. (*E*) Lipid-droplet accumulation. Cells were stained with Oil Red O after 9 days in culture. (*F–I*) Adipocyte differentiation marker mRNAs: (*F*) *Pparg* mRNA, (*G*) *Cebpa* mRNA, (*H*) *Adipoq* mRNA, and (*I*) *Fabp4* mRNA.

**Fig. 4.** Defective calvarial mineralization and osteoblast differentiation in *Ddr2*$^{slie/slie}$ mice are related to reduced RUNX2 phosphorylation. (*A, B*) Micro–CT (µCT) analysis of calvaria from newborn mice. (*A*) Representative µCT images. (*B*) Calculation of total bone volume (BV, $mm^3$). (*C–I*) Osteoblast differentiation. Calvarial osteoblasts were isolated from 12-week-old wild-type (WT) or homozygous *Ddr2*$^{slie/slie}$ female mice and grown in osteogenic medium for the times indicated. (*C*) Alizarin Red staining of 2-week-old calvaria cell cultures. (*D–F*) Osteoblast differentiation marker mRNAs: (*D*) *Runx2* mRNA, (*E*) *Bglap2* mRNA, and (*F*) *Ibsp* mRNA. (*G–I*) Western blot quantitation of DDR2, phosphorylated RUNX2, total RUNX2, phosphorylated ERK1/2, and total ERK1/2. (*J-L*) Analysis of stable cell lines from WT and *Ddr2*$^{slie/slie}$ mice expressing control vector (GFP), WT RUNX2, phosphorylation site mutant RUNX2 (RUNX2 S301,319A; SA), or phosphorylation site mimetic RUNX2 (RUNX2 S301,319E; SE). Stable cell lines were established using lentivirus transduction as described in Materials and Methods, and RUNX2 protein levels were measured by Western blotting (*J*). *Bglap2* (*K*) and *Ibsp* (*L*) mRNAs

Author Manuscript

were measured after growth in osteoblast differentiation conditions. $n$ = 8/group; statistically significant at *$p < 0.01$.

Fig. **5.** Reciprocal control of RUNX2 and PPARγ transcriptional activity by DDR2-dependent phosphorylation. (*A, B*) RUNX2 regulation. COS7 cells were transfected with a RUNX2 reporter plasmid (6OSE2-Luc) and expression vectors encoding wild type (WT) (Runx2-WT) or phosphorylation site mutant RUNX2 (Runx2 S301A/S319A), and empty vector (EV), WT, or constitutively active (CS) DDR2. (*A*) Normalized luciferase activity. (*B*) Immunoblot of RUNX2-S319-P, total RUNX2, P-ERK, and total ERK. Values under each lane indicate ratios or P-RUNX2/total RUNX2 and P-ERK/total ERK as measured by densitometry. (*C, D*) PPARγ regulation**.** Cells were transfected with PPARγ reporter/RXR combination (PPRE-Luc) as described in Materials and Methods, together with expression vectors encoding WT (PPAR-WT) or phosphorylation site mutant PPARγ (PPAR-S112AA) and EV, WT, or CS DDR2. (*C*) Normalized luciferase activity. (*D*) Immunoblot of PPARγ-S112-P, total PPARγ, P-ERK, and total ERK.

Author Manuscript

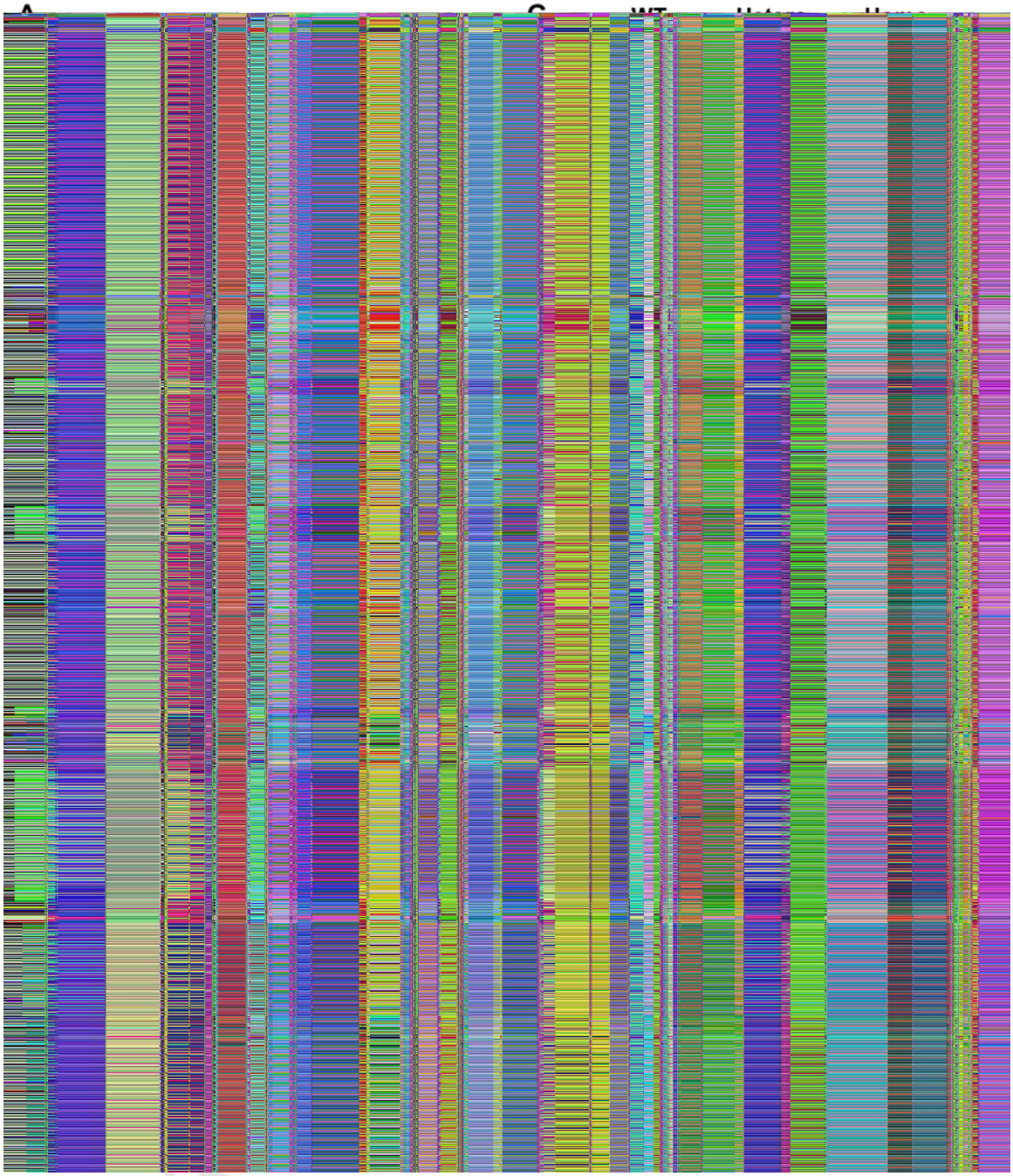

**jbmr2893-fig-0001 .**

**jbmr2893-fig-0002 .**

Author Manuscript

**jbmr2893-fig-0003 .**

Author Manuscript

**jbmr2893-fig-0004 .**

Author Manuscript

**jbmr2893-fig-0005 .**

Author Manuscript